

Estimation of Vegetation Water Content From the Radar Vegetation Index at L-Band

Yuancheng Huang, Jeffrey P. Walker, Ying Gao, Xiaoling Wu, and Alessandra Monerri

Abstract—Information on vegetation water content (VWC) is important in retrieving soil moisture using microwave remote sensing. It can be also used for other applications, including drought detection, bushfire prediction, and agricultural productivity assessment. Through the Soil Moisture Active Passive (SMAP) mission of the National Aeronautics and Space Administration, radar data may potentially provide the VWC information needed for soil moisture retrieval from the radiometer data acquired by the same satellite. In this paper, VWC estimation is tested using radar vegetation index (RVI) data from the third SMAP airborne Experiment. Comparing with coincident ground measurements, prediction equations for wheat and pasture were developed. While a good relationship was found for wheat, with $r = 0.49, 0.62,$ and 0.65 and root-mean-square error (RMSE) = $0.42, 0.37,$ and 0.36 kg/m^2 , the relationship for pasture was poor, with $r = -0.06, -0.14,$ and -0.002 and RMSE = $0.15, 0.15,$ and 0.15 kg/m^2 , for 10-, 30-, and 90-m resolutions, respectively. These results suggested that RVI is better correlated with VWC for vegetation types having a greater dynamic range. However, the results were not as good as those from a previous tower-based study ($r = 0.98$ and RMSE = 0.12 kg/m^2) over wheat. This is possibly due to spatial variation in vegetation structure and surface roughness not present in tower studies. Consequently, results from this study are expected to more closely represent those from satellite observations such as SMAP, where large variation in vegetation and environment conditions will be experienced.

Index Terms—Microwave remote sensing, radar vegetation index (RVI), soil moisture active passive experiment (SMAPEx), vegetation water content (VWC).

I. INTRODUCTION

VEGETATION water content (VWC) is an important parameter in sustainable land and water management, as it can be used in assessing agricultural productivity and predicting drought and bushfire [1]–[5]. Moreover, it plays a significant role in the retrieval of soil moisture using microwave remote sensing, which further supports applications such as weather and climate forecasting [6] and flood and landslide prediction [7]. An ability to gain accurate estimation of VWC is therefore critical.

Manuscript received October 2, 2014; revised February 23, 2015; accepted June 26, 2015. This study was conducted within the framework of the SMAPEx Project funded by the Australian Research Council under Grant DP0984586 and Grant LE0882509.

The authors are with the Department of Civil Engineering, Monash University, Vic. 3800, Australia (e-mail: yhua120@gmail.com; jeff.walker@monash.edu; ying.gao@monash.edu; xiaoling.wu@monash.edu; sandra.monerri-belda@monash.edu).

Color versions of one or more of the figures in this paper are available online at <http://ieeexplore.ieee.org>.

Digital Object Identifier 10.1109/TGRS.2015.2471803

There are currently two main approaches in estimating VWC. The conventional approach uses optical remote sensing measurements to produce large-scale maps based on spectral indexes, such as the normalized difference vegetation index (NDVI) or the normalized difference water index (NDWI) [8]–[10]. This approach can provide an estimation of VWC with root-mean-square error (RMSE) ranging from 0.40 to $0.55 \text{ kg} \cdot \text{m}^{-2}$ for cereal grains and around $0.30 \text{ kg} \cdot \text{m}^{-2}$ for grasslands [11]. However, the approach is significantly affected by atmospheric conditions and solar illumination at the time of satellite overpass [12], [13].

A recently proposed alternative has used active microwave remote sensing, otherwise referred to as radar. Compared with optical sensors, the main advantages of radar are that 1) it can penetrate clouds and acquire data regardless of time of day or weather conditions, and 2) at appropriate frequencies, radar signals can pass through vegetation canopy, allowing observation of the underlying surface [14], [15]. Active microwave observations can be also used to provide complementary information on vegetation properties, such as leaf area index, to enhance the results obtained from optical observations when limited data with an optical sensor are available [16]. However, radar measurements are also sensitive to surface roughness, topographic features, and vegetation structures, which means that acquisition of VWC from a single-frequency single-polarization backscattering observation is difficult [15].

The radar vegetation index (RVI) developed by Kim and VanZyl [17] is a simple function of radar backscatter coefficients, which includes a unique combination of all polarizations. Compared with other radar-based variables, including backscattering cross section, eigenvalues, and correlation between polarimetric channels, this polarimetric index is less sensitive to variation in both incidence angle and environmental conditions [17]. Thus, it is expected to be most suitable for estimating vegetation properties such as VWC [18]. While the RVI has been shown to generally capture vegetation patterns well, it is particularly vulnerable to errors in the calibration offset term over lightly vegetated regions [19]. However, in highly vegetated regions, which are of arguably greater interest in studies using RVI, the problem is significantly reduced [19].

Kim *et al.* [14], [20] recently undertook tower-based field studies in South Korea and subsequently proposed relationships between VWC and RVI. The experiments were conducted over a paddy field of $22 \text{ m} \times 31 \text{ m}$, a soybean field of $25 \text{ m} \times 32 \text{ m}$, and a wheat field of $20 \text{ m} \times 40 \text{ m}$, using polarimetric measurements from an L-band scatterometer mounted on a stationary platform above the fields, with a fixed incidence angle of 40° . Consequently, the study presented here tests the proposed

relationship between VWC and RVI using independent data from the third Soil Moisture Active Passive Experiment (SMAPEX-3), which was designed to provide prelaunch calibration and validation for the Soil Moisture Active Passive (SMAP) mission [21].

II. DATA SETS

The SMAP prelaunch calibration and validation activities SMAPEX consisted of a series of three airborne field campaigns, conducted across a 38 km \times 36 km study area in the Yanco region within the Murrumbidgee catchment, Australia (latitude 34°40.23' S to 35°0.76' S; longitude 145°58.84' E to 146°21.28' E). The Yanco region is a relatively flat agricultural area composed of irrigated cropland and semiarid grassland. The radar data utilized in this study were collected by the airborne Polarimetric L-band Imaging Synthetic aperture radar (PLIS), supported by ground vegetation sampling for five types of vegetation—wheat, pasture, barley, lucerne, and canola.

Beginning on September 3, 2011, the three-week-long SMAPEX-3 campaign covered a range of soil wetness and vegetation conditions. A variety of airborne data, including active and passive microwave, were collected and used as scaled replicates of data that will be available from SMAP, to develop the mathematical algorithms for soil moisture retrieval and downscaling. Full details about the campaign can be found in the SMAPEX-3 workplan [21].

A. Airborne Data

In SMAPEX-3, radar measurements were made from a small experimental aircraft from a height of 3000 m over the study area. With the PLIS radar installed, the aircraft provided ground backscatter information at 10-m resolution, for subsequent simulation of the radar data that will be available from SMAP [22]. Given a 2.2-km-wide swath on each side of the aircraft, with incidence angle ranging from nominally 15° to 45°, the ten flight lines, as shown in Fig. 1, were designed to provide full coverage of the entire study area.

Composed of two antennas and an RF unit (left and right looking), the PLIS measured L-band backscatter at all polarizations, including HH, VV, HV, and VH. Each antenna was 28.7 cm \times 28.7 cm \times 4.4 cm in size, mounted under the fuselage of the aircraft. Inclined at an angle of 30° from the horizontal, the paired antennas were able to achieve a cross-track swath of $\pm 45^\circ$, with a 1.6-km nadir gap. The measured gain of each antenna was 9 dB, with an output frequency of 1.26 GHz. More details on the PLIS system can be found in [23].

The PLIS system was calibrated using measurements from six trihedral passive radar calibrators (PRCs) deployed across the radar swath in a homogeneous grass field, as well as measurements over a forest area. All targets were imaged daily at both the beginning and end of each flight to check for any calibration drift. Data acquired from the forest area were used to calculate the cross-polarized channel imbalances, whereas copolarized channel imbalances were estimated using the PRC data. Absolute radiometric calibration, defined as the difference between the measured PRC backscattered power and the theoretical radar cross section for the PRCs, was calculated

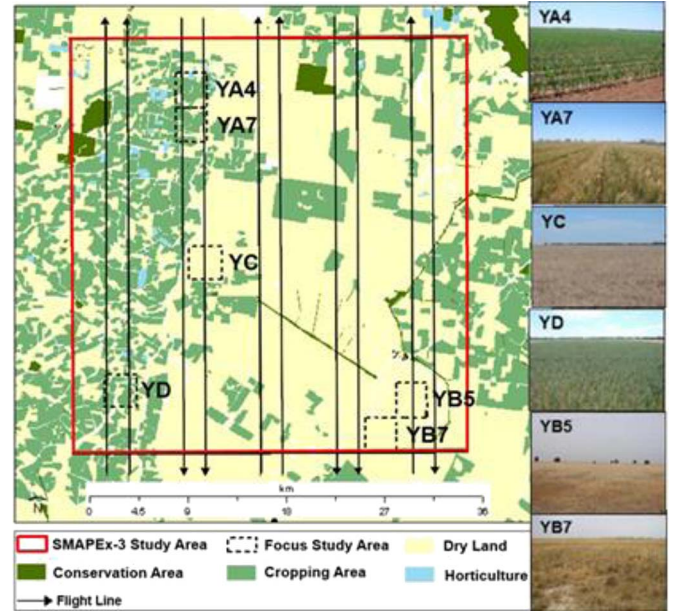


Fig. 1. Layout of the SMAPEX-3 study area indicating the six focus areas and the ten flight lines, from [21].

as 0.93 dB on average with a standard deviation of 0.8-dB relative radiometric accuracy [24]. By comparing data from all targets from the start and end overpasses, repeatability was calculated as approximately 0.9-dB RMSE at copolarization and 1.4 dB at cross-polarization, which meet the requirement of radar measurement accuracy for SMAP [22].

As data from the SMAPEX-3 were collected at incidence angles between 15° and 45°, they were converted to the equivalent values that would be observed at 40° by SMAP [25]. The method used is a nonlinear approach that matches the cumulative frequency distribution of observations at the observing incidence angle with the cumulative frequency of observations at a reference angle and has been shown to provide superior results to other normalization methods [25]. The normalized data used in this study were estimated by Wu *et al.* [22] to have accuracy of around 3.2, 1.8, and 0.8 dB at 10-m, 100-m, and 1-km resolutions, respectively.

B. Ground Vegetation Sampling

Ground vegetation sampling was conducted daily within 10-m pixels at one or more of the six 2.8 km \times 3.1 km focus areas across the region, as shown in Fig. 1 [21]. Each of these focus areas was equivalent to a radar-sized pixel from the SMAP grid and was selected to characterize all major types of vegetation present within the study area, including wheat, pasture, barley, lucerne, and canola. Located in the eastern part of the study area, the “YA” and “YD” areas presented a mix of flood irrigated and dryland cropping areas and grazing areas, where higher spatial variability and wetter soil conditions were observed. Located in flat regions characterized by uniform grasslands, the “YB” and “YC” areas presented drier and more uniform conditions. These areas were sampled concurrently with airborne observations on a rotational basis, with relatively fewer sampling points in the grassland sites.

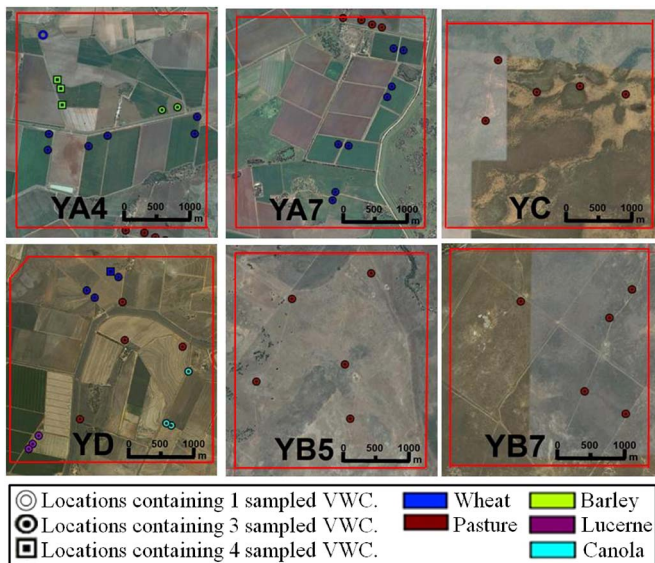


Fig. 2. Locations for vegetation sampling in each of the six focus areas. Three indicators—hollow circle, solid circle, and solid square—represent the different numbers of samples collected in each location during the SMAPEX-3 campaign; five colors—blue, red, green, purple, and aqua—represent the vegetation types.

During the field campaign, vegetation was sampled using a $0.5\text{ m} \times 0.5\text{ m}$ quadrant that was randomly placed on the ground within the area to be sampled. All above-ground biomass within the quadrant was removed, doubled bagged, and then sealed with rubber bands to ensure no moisture loss. The samples were processed daily to obtain a wet weight before being placed in a dehydrator to dry at 65°C for two to three days until a constant weight was reached. To avoid any moisture absorbed from the air, which would affect the accuracy of the measurement, all dry samples were immediately weighted once they were taken out of the dehydrator. Knowing the difference in weight between wet and dry samples allowed the VWC to be calculated.

To accurately track the temporal changes in VWC and biomass, measurements were repeated weekly at the same locations over the three-week period. As shown in Fig. 2, a total of 19, 23, 5, 3, and 3 locations was chosen for sampling of wheat, pasture, barley, lucerne, and canola across the six focus areas, giving a total of 55, 69, 18, 9, and 9 measurements for each vegetation type. However, as flights were not scheduled daily during the three-week experiment, the number of samples available in this study was significantly reduced. Only 30, 47, 5, 3, and 3 coincident measurements were used. Fig. 3 shows the distribution of the sampled VWC used in this study. For wheat, VWC varied over a large range, being from 0.4 to 2.6 kg/m^2 . For pasture, a limited dynamic range of VWC was observed across the six focus areas, with 85% of VWC being less than 0.4 kg/m^2 . For barley, lucerne, and canola, as only a limited number of VWC were available, data were presented for comparative purposes only. A complete summary of dominant vegetation types, ground sampling measurements, and dynamic ranges of VWC for each focus areas is shown in Table I.

Due to differences in field conditions over the entire study area, it is also important to appreciate the spatial variation in VWC measurements used in this study. The standard deviation

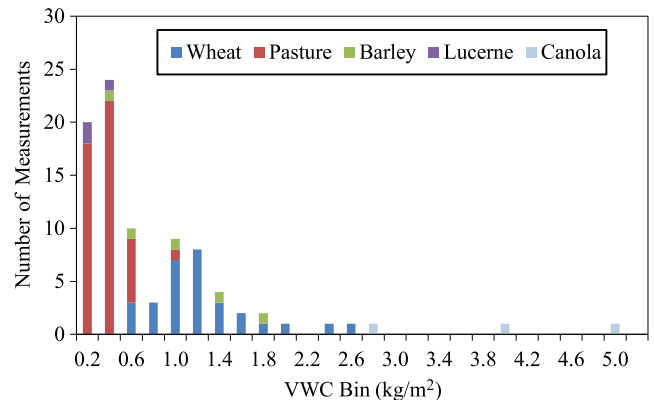


Fig. 3. Distribution of sampled VWC collected from six focus areas across the SMAPEX-3 study area.

TABLE I
SUMMARY STATISTICS OF THE SMAPEX-3 GROUND MEASUREMENTS FOR DOMINANT VEGETATION TYPES IN EACH FOCUS AREA

Focus Areas	Vegetation Types	Total Samples	Coincident Samples	VWC (kg/m^2)
YA4	Wheat	19	10	0.72 - 2.52
	Pasture	12	8	0.12 - 0.95
	Barley	18	5	0.16 - 1.85
YA7	Wheat	24	16	0.51 - 1.59
YC	Pasture	15	10	0.07 - 0.49
YD	Wheat	12	4	1.03 - 1.87
	Pasture	12	4	0.07 - 0.31
	Lucerne	9	3	0.11 - 0.34
	Canola	9	3	2.78 - 7.71
YB5	Pasture	15	10	0.15 - 0.37
YB7	Pasture	15	15	0.20 - 0.55
	Total	160	88	

Total samples: total number of sampling measurements; coincident samples: number of measurements collected concurrently with airborne data acquisition.

on collocated measurements representing the same pixel and time is 0.27 and 0.12 kg/m^2 for wheat and pasture, respectively, averaged over the three-week period. While the VWC for pasture was relatively uniform spatially, it is not surprising that wheat experienced a greater variation due to irrigation and differences in growth rate. Again, data for barley, lucerne, and canola are not presented here due to the limited number of measurements available.

III. METHODOLOGY

In order to accurately estimate VWC from radar across a range of vegetation types, the approach should be minimally affected by variation in vegetation structure, incidence angle, and environmental conditions, such as surface roughness. It

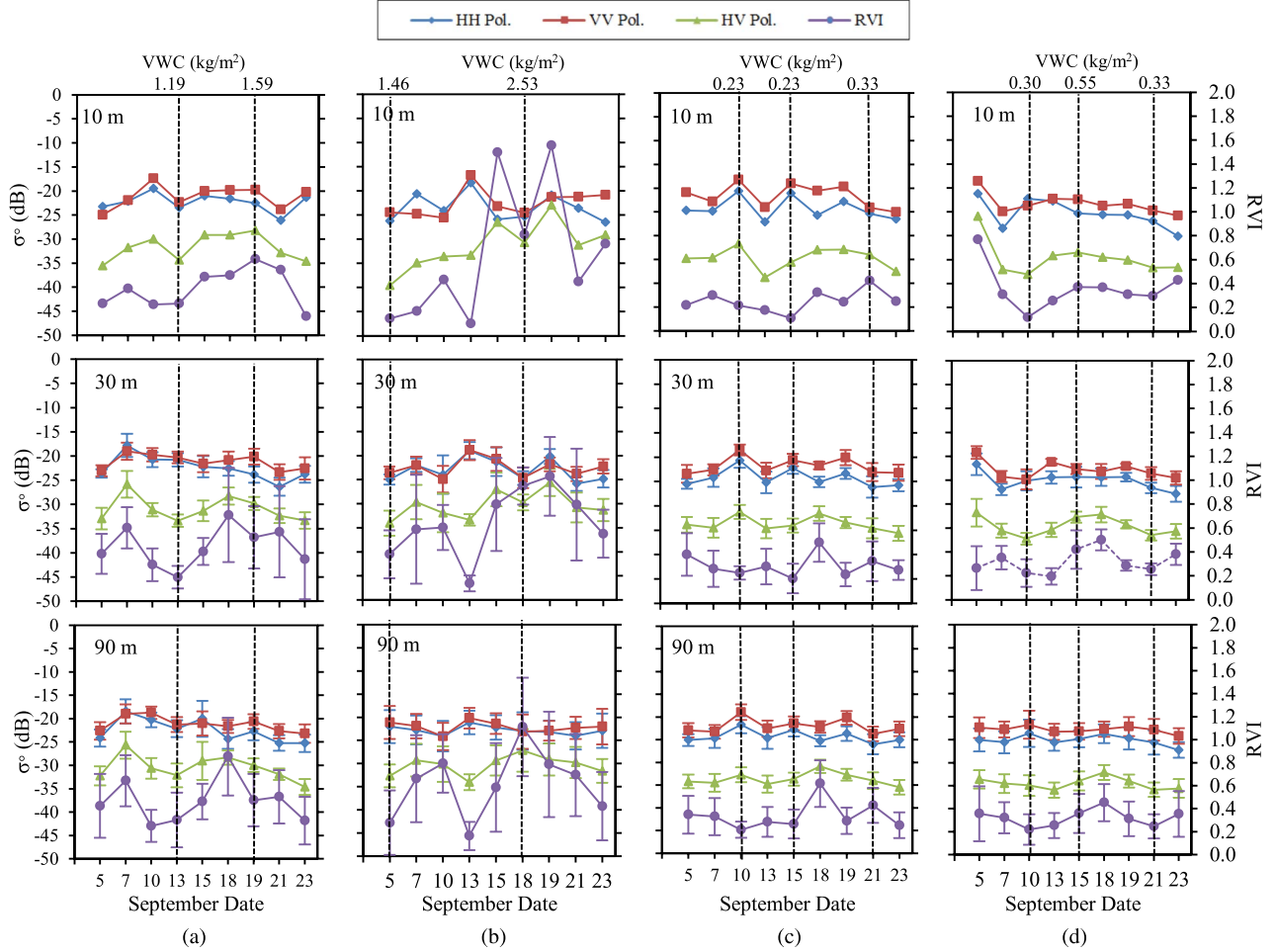


Fig. 4. Time series of L-band backscatter coefficient σ^o and RVI plotted daily at four points of sampling for (a) and (b) wheat and (c) and (d) pasture, with radar data resolution and VWC as indicated in each panel. Each data point represents the averages and standard deviations of the backscatter coefficients aggregated from 10 m to 30- and 90-m resolutions. Data are observed at a range of incidence angles and converted to equivalent values as observed at 40° by angle normalization.

has been proposed that RVI meets this requirement [17] and is therefore tested as a potential radar-based quantity that may be directly related to VWC. The RVI can be calculated by

$$\text{RVI} = \frac{8\sigma_{\text{HV}}}{\sigma_{\text{HH}} + \sigma_{\text{VV}} + 2\sigma_{\text{HV}}} \quad (1)$$

where σ_{HV} is the cross-polarization backscattering coefficient, and σ_{HH} and σ_{VV} are the copolarization backscattering coefficients, represented in power unit. RVI measures the randomness of scattering and ranges between 0 and 1, with near 0 for a smooth bare soil surface and a larger number for increasing VWC. Supported by ground vegetation sampling, the relationship between sampled VWC and its corresponding RVI obtained from the PLIS radar was examined, using alternate regression fits. Linear regression, which gave the best results for the relationship, was found most suitable and therefore adopted in this study. Moreover, the RMSE was also calculated and compared with optical results.

For high-resolution observations, the ratio of received-to-reflected energy for vegetated surfaces can be influenced to a great extent, depending on ground surface roughness, soil moisture, radar incidence angle, and vegetation structure, as well as VWC. Moreover, speckle noise in radar data acquisition

is likely, and thus, errors carried in the RVI derivation could be considerable, which may then translate to a poor relationship between VWC and RVI. Consequently, steps were taken to minimize these errors by aggregating the airborne backscattering coefficients from 10-m resolution to 30- and 90-m resolutions at 10-m increments. Resolutions of 30 and 90 m are equivalent to 9 and 81 pixels at a resolution of 10 m, and spatially averaged RVI can be therefore achieved by taking the average of adjacent backscattering coefficients and calculating the RVI. This resulting RVI was then matched with corresponding VWC to assess impacts on the relationship.

In the case of effects due to errors in the normalization process, RVI was also derived from the original nonangle corrected backscatter observations and compared against sampled VWC for separate incident angle bins. Results are compared with those from the angle normalized results.

IV. RESULTS

A. Time Series of Analysis Using 40° Incidence Angle Corrected Data

Fig. 4 shows example time series of backscatter coefficients recorded during SMAPEX-3 to assess the response of the

TABLE II
LINEAR REGRESSION OF VWC AND RVI AT 10-, 30-, AND 90-M RESOLUTIONS (40° ANGLE CORRECTED)

Type	Resolution	Regression Equation	r	RMSE	p-value	Size
Wheat	10 m	$y = 0.71x + 0.86$	0.49	0.42	0.006	30
	30 m	$y = 0.98x + 0.74$	0.62	0.37	0.0002	
	90 m	$y = 1.01x + 0.68$	0.65	0.36	0.0001	
	Kim et al	$y = 14.36x - 5.51$	0.98	0.12	-	-
Pasture	10 m	$y = -0.04x + 0.27$	-0.06	0.15	0.698	47
	30 m	$y = -0.13x + 0.31$	-0.14	0.15	0.338	
	90 m	$y = -0.002x + 0.26$	0.00	0.15	0.988	

y: VWC (kg/m²); x: RVI r: correlation coefficient; RMSE: root mean square error (kg/m²); size: sample size.

different radar channels at different resolutions to changes in VWC. The graphs also include the time series of calculated RVI over the same period. In order to present the range of conditions encountered in the SMAPEX study area, sampling data from a point in focus area YA7 and YA4 were chosen for wheat, and two points in focus area YB7 were chosen for pasture. Note that all data presented in the graphs were 40° angle corrected in accordance with the SMAP viewing angle and did not include those for barley, lucerne, and canola due to the limited number of samples available. For the wheat field, both the backscatter coefficient and RVI exhibited a positive correlation to VWC, with σ_{HV} and RVI increasing in response to the increase in VWC. However, compared with the change in σ_{HV} , a more sensitive response was observed in RVI, demonstrating the potential for using RVI to estimate VWC in the context of soil moisture retrieval. It was also observed that the difference between σ_{HV} and σ_{VV} decreased as VWC increased. This comes mainly as the result of an increase in canopy volume scattering at HV polarization as the crops grew in size and increased in VWC. Moreover, the scatterplots of radar data at 30- and 90-m resolutions were very similar, suggesting that the speckle noise contained in the radar data has been minimized after aggregation. For pasture, while backscatter coefficients exhibited a positive correlation to VWC in the experiment field where higher VWC was observed [see Fig. 4(d)], they did not exhibit the same correlation as expected in the field where sampled VWC was relatively lower [see Fig. 4(c)]. Conversely, a negative correlation was observed to persist after backscatter coefficients were aggregated from 10-m resolution to 30- and 90-m resolutions, particularly for σ_{HV} , which is generally more related to volume scattering of vegetation compared with σ_{HH} and σ_{VV} . However, this might be the result of radar data being affected mainly by other factors, such as surface roughness and soil moisture, since pasture had a relatively low VWC (0.23–0.33 kg/m²). In addition, the differences between σ_{HH} , σ_{VV} , and σ_{HV} were fairly constant throughout the experiment, and this could be a result of an already well-developed pasture field where environment conditions were relatively consistent. However, notice that RVI still exhibits a positive correlation to VWC with increased RVI, which again shows the potential for using RVI to estimate VWC.

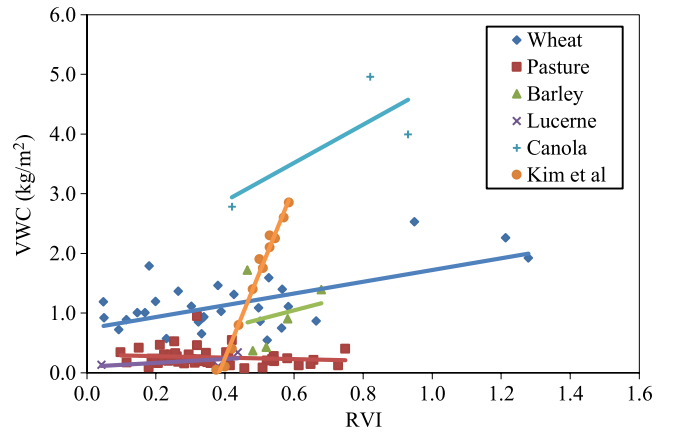


Fig. 5. Relationship between VWC and RVI observed using 40° angle normalized data at 30-m resolution.

B. VWC Estimation Using 40° Incidence Angle Corrected Data

Five major vegetation types were observed in the SMAPEX-3 study area. While there were only a limited number of vegetation samples available for barley, lucerne, and canola, these are still presented for comparative purposes.

Table II summarizes the results from SMAPEX-3 for spatial resolutions from 10 to 90 m with normalized RVI, together with those from the recent study by Kim *et al.* [20]. For wheat, the slope of the regression line increases with decreasing spatial resolutions, from 0.71 at 10-m resolution to 1.01 at 90-m resolution, with a corresponding increase in correlation coefficient by about 34% and reduction in RMSE by 13%, in magnitude. For pasture, there was a negative slope for all resolutions, with low and inconsistent correlation coefficients. In short, the difference in results between resolutions from 30 to 90 m was small, and thus, 30-m resolution data are presented and used hereon as a compromise between minimizing speckle noise and the spatial scale of ground measurement.

More important, the relationship proposed by Kim *et al.* was not found to be robust, with their correlation coefficient of close to 1 being much higher than that found here, although data were processed for the same 40° incidence angle. This is further highlighted in Fig. 5, where the relationship at 30-m

resolution between sampled VWC and the corresponding normalized RVI is shown for the different vegetation types and compared with those from the study by Kim *et al.* It is shown that, for wheat, an increase in RVI had a corresponding increase in VWC overall and that data were evenly distributed around the regression line, yielding a good relationship between VWC and RVI. However, the slope of this relationship was distinctively different to that developed by Kim *et al.*

For pasture, there was only a small change in VWC with increase in RVI, resulting in a flat regression line and a poor relationship between VWC and RVI, which was unexpected. However, upon reflection, this is not surprising, considering the very small dynamic range of VWC for pasture fields during the three-week-long SMAPEX-3 (average of 0.26 kg/m^2 and standard deviation of 0.15 kg/m^2), whereas the fields of other vegetation types provided had a wider range of VWC conditions. Moreover, the radar short-term calibration stability and the within-field spatial variability might also impact the correlation between VWC and RVI, when the analysis is subjected to very small dynamic ranges of VWC. However, the grasslands can be easily distinguished from other vegetation types, and while the correlation is poor, the approach might be sufficient to estimate the VWC of grasslands given the relatively small RMSE.

C. VWC Estimation Using Native Data for Different Incidence Angle Ranges

To check for possible effects due to normalization errors, RVI derived from nonangle corrected backscatter was also examined against VWC. Nonangle normalized RVI were divided into three 10° angle groups. Again, data for barley, lucerne, and canola were presented for comparative purposes only, due to the limited number of vegetation samples available.

Fig. 6 shows the relationship between sampled VWC and observed RVI at 30-m resolution according to incidence angle groupings. For wheat, the results demonstrated a good relationship in the 15° – 25° angle range with evenly distributed data points around the linear fit, and sloping upward. Table III summarizes the relationship between VWC and RVI for all coincident vegetation data for the angle groupings tested. Due to the limited number of samples available, data for the 35° – 45° range are not considered in the discussion and presented for comparative purposes only. For the other two groups, it was found that the slope of the regression line and the correlation coefficient were relatively small ($m = 1.65$ and 0.76 , $r = 0.46$ and 0.26 , respectively, for groups 15° – 25° and 25° – 35°); in addition, the RMSE values were quite similar for each angle bin and for the normalized angle results. For the 25° – 35° angle range, the smaller slope for the linear fit suggests that the RVI could be less sensitive to VWC in this angle range, or that the relationship between VWC and RVI could be affected more by other environment factors. After normalizing radar backscatters to those equivalently observed at 40° , a better relationship between VWC and RVI was found, with $r = 0.62$. This shows that 40° angle normalization was effective to improve correlation of RVI to VWC. For pasture, regression lines for all angles were nearly flat, which means

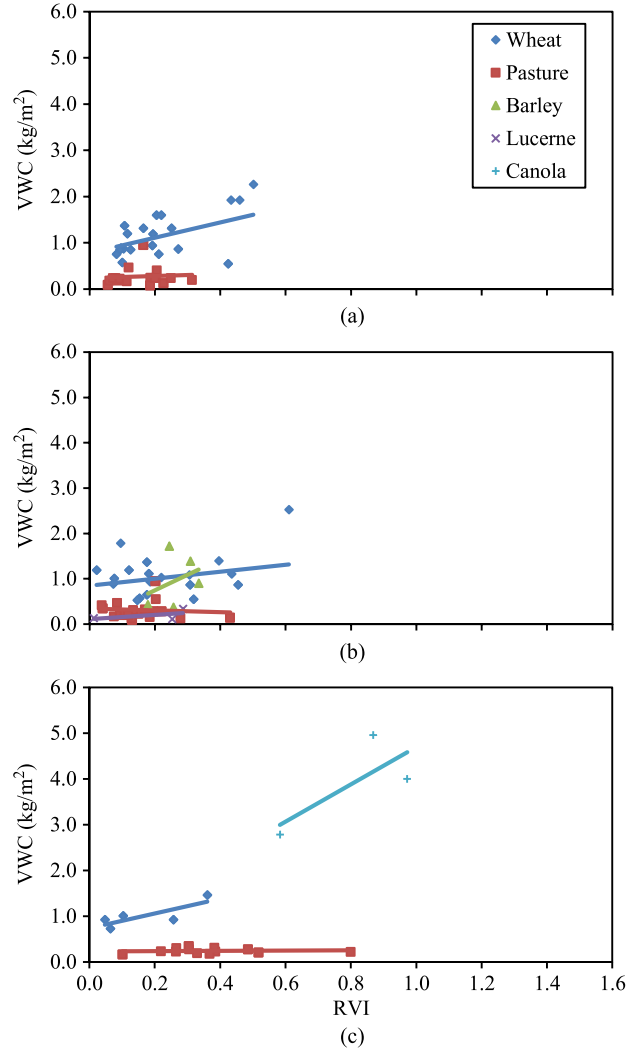


Fig. 6. Relationship between VWC and RVI observed for data in angle range of (a) 15° – 25° , (b) 25° – 35° , and (c) 35° – 45° at 30-m resolution for wheat, pasture, barley, lucerne, and canola.

that VWC and RVI were again not well correlated, possibly due to the low dynamic range of VWC. While the associated RMSE varied significantly across different angle groups, it was equivalent to that from normalized data. Consequently, the normalized RVI results are believed to be representative of what would have been achieved if observed directly at 40° , and therefore, this analysis may be directly applicable to SMAP.

V. DISCUSSION

Compared with the study conducted by Kim *et al.* [20], which demonstrated a direct-proportional relationship between VWC and RVI ($r = 0.98$ and $\text{RMSE} = 0.12 \text{ kg/m}^2$ for wheat), the proposed relationship from this study was not so robust ($r = 0.62$ and $\text{RMSE} = 0.37 \text{ kg/m}^2$). This may be due to the differences in data acquisition methods. In SMAPEX-3, the three-week-long experiment was conducted across a $38 \text{ km} \times 36 \text{ km}$ region and was timed to capture a phase of intensive growth of Austral spring crops. The region presented a mix of irrigated and dryland cropping areas, where surface

TABLE III
LINEAR REGRESSION OF VWC AND RVI AT DIFFERENT INCIDENCE ANGLES (30-m RESOLUTION, NOT ANGLE CORRECTED)

Type	Angle Group	Regression Equation	r	RMSE	p-value	Size
Wheat	15°-25°	$y = 1.65x + 0.78$	0.46	0.37	0.004	37
	25°-35°	$y = 0.76x + 0.85$	0.26	0.39	0.148	32
	35°-45°	$y = 1.61x + 0.74$	0.8	0.15	0.006	10
Pasture	15°-25°	$y = 0.22x + 0.24$	0.07	0.24	0.777	21
	25°-35°	$y = -0.19x + 0.34$	-0.09	0.21	0.668	27
	35°-45°	$y = 0.03x + 0.23$	0.09	0.06	0.744	17

y: VWC (kg/m^2); x: RVI; r: correlation coefficient; RMSE: root mean square error (kg/m^2); size: sample size.

roughness, soil moisture, and biomass density were expected to vary significantly. Moreover, radar data were acquired by an airborne sensor at 3000-m height with $10\text{ m} \times 10\text{ m}$ footprints on the ground. In contrast, the experiment of Kim *et al.* was for a single wheat field of $20\text{ m} \times 30\text{ m}$, where soil conditions were very consistent through time. From seeding to full maturity, their 164-day-long study covered an entire growing season, with radar data acquired from a stationary platform with an incident angle of 40° at a height of 4 m. Therefore, considering the variations in size and conditions of the experimental fields, as well as the techniques used to acquire radar data, it should not be surprising that there could be a larger error of estimation involved in the SMAPEX-3 data relative to the study of Kim *et al.* However, the large difference in slope of the relationship still requires some explanation. Five aspects were recognized to have possibly impacted on the results.

First, random fluctuations in radar signals returned from an object can lead to considerable speckle noises. However, reducing the spatial resolution will have minimized these errors. Such errors should not exist in the tower data due to the ability to multilook through time rather than space. While decreased resolution reduced the RMSE, it did not considerably impact on the slope.

Second, there was only a limited number of vegetation samples collected in SMAPEX-3. While vegetation sampling was designed in a way that VWC samples were representative of the surrounding $10\text{ m} \times 10\text{ m}$ area where sampling was made, the same sampled VWC was then used to represent the larger areas when resolution was reduced. This may lead to greater uncertainty in the VWC estimates, but again, this is not expected to impact the slope of the relationship.

Third, the transformation function that converts backscatter coefficients observed at a variety of incidence angles to the equivalent value at 40° was not developed for application at high spatial resolution. Errors of approximately 3.2 dB have been found at 10-m resolution and 1.8 dB at 100-m resolution, and consequently, the RVI from nonnormalized angles may be in error. As a result, the differences in slope of the relationship might in part be attributed to angular normalization to 40° , particularly from observations at low incidence angles where slight difference in polarization response is expected.

Fourth, cropping areas in the SMAPEX-3 where wheat was sampled presented a large variety of growth stages and veg-

TABLE IV
REGRESSION OF VWC AND OPTICAL VEGETATION INDICES, FROM [11]

Type	Index	Regression Equation	r	RMSE
Cereal Grains	NDVI	$y = 0.078 e^{3.510x}$	0.77	0.50
	NDWI ₁₆₄₀	$y = 2.45x + 0.57$	0.75	0.43
Grassland	NDVI	$y = 0.017 e^{5.866x}$	0.72	0.33
	NDWI ₁₆₄₀	$y = 1.16x + 0.45$	0.45	0.30

y: VWC (kg/m^2); x: respective index; r: correlation coefficient; RMSE: root mean square error (kg/m^2).

etation structures, in terms of plant height (33.0–73.3 cm), density (8–16 plants per meter), and row spacing (19–33 cm). This means that randomly oriented scattering particles in crop plants could vary significantly from field to field in SMAPEX-3, whereas this was not the case in Kim *et al.*, where vegetation structure was relatively consistent over the experimental area. As radar backscatter is strongly affected by vegetation structure [26]–[28], there could be variation in backscatter even for similar VWC.

Finally, variation in soil moisture and surface roughness impacts the backscatter in addition to vegetation. A major difference between these two studies is the constant (or slowly varying) roughness in the case of a fixed tower looking at the same patch of soil, whereas there will have been large variations in roughness conditions and look angles relative to row directions in the case of airborne data. Consequently, it is this variation in roughness that seems to contribute the most to the discrepancy between the results here and those by Kim *et al.* Moreover, these results will therefore more closely represent those expected from satellites such as SMAP, where large variations in surface roughness will be experienced.

It is also important to contrast these results with those from other techniques. Compared with a recent synthesis study on the use of optical data to estimate VWC for the same study site (RMSE ranged from 0.43 to 0.50 kg/m^2 for cereal grains, as shown in Table IV), radar-based RVI has shown an improvement in VWC estimation for vegetation types having a greater dynamic range (corresponding RMSE reduced to 0.36–0.42 kg/m^2 for wheat). However, for vegetation types having lower VWC, the correlation of RVI with VWC ($r = -0.06$ – 0.00 for pasture) is not as robust as that of optical vegetation indexes ($r = 0.45$ – 0.72 for grassland), mainly due to the effects of surface roughness. While the use of radar data

is a promising approach for VWC estimation, both approaches will require *a priori* information on the vegetation type, due to the different empirical relationships that have been found.

VI. CONCLUSION

The VWC is an important parameter in retrieving soil moisture from radiometer measurements and can be also used in a range of applications. There are two major approaches in estimating VWC, one involving the use of optical sensors and the other being active microwave remote sensing. In this paper, radar data acquired from the SMAPEX-3 field campaign were converted to RVI and plotted against ground-measured VWC.

Five types of vegetation were identified in SMAPEX-3, including wheat, pasture, barley, lucerne, and canola, but due to the limited number of samples, only wheat and pasture have been rigorously assessed here. Moreover, results are presented at 30-m spatial resolution as a compromise between minimizing speckle noise and the spatial scale of ground measurement. Comparison was also made with nonnormalized angle observations to confirm that angle normalization had not adversely affected the accuracy of results.

The relationship between VWC and RVI at an angle of 40° was found to have an RMSE of 0.38 kg/m^2 for wheat and 0.15 kg/m^2 for pasture at 30-m resolution. A similar study using tower data found better results, with an RMSE of 0.12 kg/m^2 for wheat. Moreover, there is a large difference in the slope of the relationships found for wheat by these two studies, likely due to differences in vegetation structure and surface roughness. Compared with optical sensors (RMSE ranging from 0.40 to 0.55 kg/m^2 for cereal grains and around 0.30 kg/m^2 for grassland), the radar-based RVI approach has shown better results. However, the apparent roughness impact may limit spatial application.

ACKNOWLEDGMENT

The authors would like to thank the participants of the SMAPEX campaigns, particularly those involved in measurements of vegetation properties. They would also like to thank the Faculty of Engineering of Monash University for providing an undergraduate research opportunity for Y. Huang.

REFERENCES

- [1] E. R. Hunt, Jr., L. Li, M. T. Yilmaz, and T. J. Jackson, "Comparison of vegetation water contents derived from shortwave-infrared and passive-microwave sensors over central Iowa," *Remote Sens. Environ.*, vol. 115, no. 9, pp. 2376–2383, Sep. 2011.
- [2] H. Lawrence *et al.*, "Comparison between SMOS Vegetation Optical Depth products and MODIS vegetation indices over crop zones of the USA," *Remote Sens. Environ.*, vol. 140, pp. 396–406, Jan. 2014.
- [3] D. M. LeVine and M. A. Karam, "Dependence of attenuation in a vegetation canopy on frequency and plant water content," *IEEE Trans. Geosci. Remote Sens.*, vol. 34, no. 5, pp. 1090–1096, Sep. 1996.
- [4] J. Penuelas, I. Filella, C. Biel, L. Serrano, and R. Save, "The reflectance at the 950–970 nm region as an indicator of plant water status," *Int. J. Remote Sens.*, vol. 14, no. 10, pp. 1887–1905, 1993.
- [5] B. C. Gao and A. F. Goetz, "Retrieval of equivalent water thickness and information related to biochemical components of vegetation canopies from AVIRIS data," *Remote Sens. Environ.*, vol. 52, no. 3, pp. 155–162, Jun. 1995.
- [6] Y. Y. Liu, A. I. J. M. van Dijk, R. A. M. de Jeu, and T. R. H. Holmes, "An analysis of spatiotemporal variations of soil and vegetation moisture from a 29-year satellite-derived data set over mainland Australia," *Water Res. Res.*, vol. 45, no. 7, 470–474, Jul. 2009.
- [7] M. Owe, R. de Jeu, and T. Holmes, "Multisensor historical climatology of satellite-derived global land surface moisture," *J. Geophys. Res.*, vol. 113, no. F1, Mar. 2008, Art. No. F01002.
- [8] T. J. Jackson and T. J. Schmugge, "Vegetation effects on the microwave emission of soils," *Remote Sens. Environ.*, vol. 52, no. 3, pp. 155–162, Jun. 1995.
- [9] C. J. Tucker, "Red and photographic infrared linear combinations for monitoring vegetation," *Remote Sens. Environ.*, vol. 8, no. 2, pp. 127–150, May 1979.
- [10] D. Chen, T. J. Jackson, F. Li, M. H. Cosh, and C. Walthall, "Estimation of vegetation water content for corn and soybeans with a normalized difference water index (NDWI) using Landsat thematic mapper data," in *Proc. IEEE Geosci. Remote Sens. Symp.*, Jul. 2003, vol. 4, pp. 2853–2856.
- [11] Y. Gao *et al.*, "Optical sensing of vegetation water content: A synthesis study," *IEEE J. Sel. Topics Remote Sens.*, vol. 8, no. 4, 1456–1464, Apr. 2015.
- [12] T. J. Jackson *et al.*, "Vegetation water content mapping using Landsat data derived normalized difference water index for corn and soybean," *Remote Sens. Environ.*, vol. 92, no. 4, pp. 475–482, Sep. 2004.
- [13] D. Chen, J. Huang, and T. J. Jackson, "Vegetation water content estimation for corn and soybeans using spectral indices derived from MODIS near- and short-wave infrared bands," *Remote Sens. Environ.*, vol. 98, no. 2/3, pp. 225–236, Oct. 2005.
- [14] Y. Kim, T. Jackson, H. Lee, and S. Hong, "Radar vegetation index for estimating the vegetation water content of rice and soybean," *IEEE Trans. Geosci. Remote Sens.*, vol. 9, no. 4, pp. 564–568, Jul. 2012.
- [15] J. P. Walker, P. Houser, and G. Willgoose, *Active Microwave Remote Sensing for Soil Moisture Measurement: A Field Evaluation Using ERS-2*. Hoboken, NJ, USA: Wiley, Aug. 2004, vol. 18, no. 11, pp. 1975–1997.
- [16] J. G. P. W. Clevers and H. J. C. van Leeuwen, "Combined use of optical and microwave remote sensing data for crop growth monitoring," *Remote Sens. Environ.*, vol. 56, no. 1, pp. 42–51, Apr. 1996.
- [17] Y. J. Kim and J. VanZyl, "A time-series approach to estimate soil moisture using polarimetric radar data," *IEEE Trans. Geosci. Remote Sens.*, vol. 47, no. 8, pp. 2519–2527, Aug. 2009.
- [18] M. Arii, J. van Zyl, and Y. Kim, "A general characterization for polarimetric scattering from vegetation canopies," *IEEE Trans. Geosci. Remote Sens.*, vol. 48, no. 9, pp. 3349–3357, Sep. 2010.
- [19] K. A. McColl, D. Entekhabi, and M. Piles, "Uncertainty analysis of soil moisture and vegetation indices using Aquarius scatterometer observations," *IEEE Trans. Geosci. Remote Sens.*, vol. 52, no. 7, pp. 4259–4272, Jul. 2014.
- [20] Y. Kim *et al.*, "Retrieval of wheat growth parameters with radar vegetation indices," *IEEE Trans. Geosci. Remote Sens.*, vol. 11, no. 4, pp. 808–812, Apr. 2014.
- [21] A. Monerris *et al.*, *The Third Soil Moisture Active Passive Experiment Workplan*. Melbourne, VIC, Australia: Monash Univ. Publisher, Aug. 2011.
- [22] X. Wu, J. P. Walker, C. Rüdiger, R. Panciera, and D. Gray, "Simulation of the SMAP data stream from SMAPEX field campaigns in Australia," *IEEE Trans. Geosci. Remote Sens.*, vol. 53, no. 4, pp. 1921–1934, Apr. 2015.
- [23] D. Gary *et al.*, "PLIS: An airborne polarimetric L-band interferometric synthetic aperture radar," in *Proc. APSAR*, 2012, pp. 1–4.
- [24] R. Panciera *et al.*, "The Soil Moisture Active Passive Experiment (SMAPEX): Towards soil moisture retrieval from the SMAP mission," *IEEE Trans. Geosci. Remote Sens.*, vol. 52, no. 1, 490–507, Jan. 2014.
- [25] N. Ye, J. Walker, and C. Rüdiger, "A cumulative distribution function method for normalizing variable-angle microwave observations," *IEEE Trans. Geosci. Remote Sens.*, vol. 53, no. 7, 3906–3916, Jul. 2015.
- [26] M. W. Whitt and F. T. Ulaby, "Radar response of periodic vegetation canopies," *Int. J. Remote Sens.*, vol. 15, pp. 1813–1848, Oct. 1993.
- [27] A. Monsivais-Huertero, I. Chenerie, K. Sarabandi, F. Baup, and E. Mougin, "Microwave electromagnetic modelling of Sahelian grassland," *Int. J. Remote Sens.*, vol. 31, no. 7, pp. 1915–1942, Dec. 2008.
- [28] D. Liu, G. Sun, Z. Guo, K. Jon Ranson, and Y. Du, "Three-dimensional coherent radar backscatter model and simulations of scattering phase center of forest canopies," *IEEE Trans. Geosci. Remote Sens.*, vol. 48, no. 1, pp. 349–357, Jan. 2010.



Yuancheng Huang received the B.E. (with first-class honors) degree in civil engineering from Monash University, Melbourne, VIC, Australia, in 2013.

During his undergraduate studies, he showed great interests in geoscience and radar remote sensing, and under the supervision of Prof. Jeffrey P. Walker, undertook a research project on estimation of vegetation water content using RVI at L-band. He continued his study in the same area after graduation and had his first academic paper published by the

IEEE. He was with Monash University at the time of writing this paper.



Jeffrey P. Walker received the B.E. degree in civil engineering and the B.Surv. (with first-class honors and University Medal) degree in 1995 and the Ph.D. degree in water resources engineering in 1999, all from The University of Newcastle, Callaghan, NSW, Australia.

He then joined the NASA Goddard Space Flight Center to implement his soil moisture work globally. In 2001, he joined, as a Lecturer, the Department of Civil and Environmental Engineering, The University of Melbourne, Melbourne, VIC, Australia,

where he continued his soil moisture work, including the development of the only Australian airborne capability for simulating new satellite missions for soil moisture. In 2010, he became a Professor with the Department of Civil Engineering, Monash University, Melbourne, where he is continuing this research. He is contributing to soil moisture satellite missions at NASA, the European Space Agency, and the Japanese Aerospace Exploration Agency, as a Science Team Member for the Soil Moisture Active Passive mission and a Cal/Val Team Member for the Soil Moisture and Ocean Salinity mission and Global Change Observation Mission - Water, respectively.



Ying Gao received the B.E. (with first-class honors) degree in civil engineering from Monash University, Melbourne, VIC, Australia, and Central South University, Changsa, China, in 2010. She is currently working toward the Ph.D. degree in civil engineering at Monash University.

She was awarded a Faculty Scholarship to continue her Ph.D. studies. She was involved in the Soil Moisture Active and Passive (SMAP) Experiments field campaigns as part of NASA's SMAP mission. Her research interests include active and passive microwave remote sensing, optical sensing of vegetation, soil moisture retrieval, and surface roughness parameterization.

and surface roughness parameterization.



Xiaoling Wu received the B.E. degree in biomedical engineering from Zhejiang University, Hangzhou, China, in 2009, and the Ph.D. degree in civil engineering from Monash University, Melbourne, VIC, Australia, in 2015. The topic of her undergraduate thesis was the development of biosensor using nanomaterial.

She is currently working as a Postdoctoral Researcher with the Department of Civil Engineering at Monash University. After graduation, she undertook a one-year research project in computer science at

the University of Copenhagen, Copenhagen, Denmark. Her current research focuses on downscaling of soil moisture using airborne radar and radiometer observations, which is expected to provide an accurate and high-resolution (> 10 km) soil moisture product, with potential benefit in the areas of weather forecasting, flood and drought prediction, agricultural activities, etc.



Alessandra Monerri received the B.E. degree in telecommunication from Universitat Politècnica de València, València, Spain, and the Ph.D. degree in telecommunication from Universitat Politècnica de Catalunya, Barcelona, Spain.

In 2006, she was a Visiting Ph.D. Student with the University of Rome "Tor Vergata," Rome, Italy. From 2007 to 2011, she was the Executive Director of SMOS Barcelona Expert Centre (the Soil Moisture and Ocean Salinity Mission Expert Centre) Barcelona. Since 2011, she has been a Research

Fellow with the Department of Civil Engineering, Monash University, Melbourne, VIC, Australia. She has extensive experience in the preparation and coordination of field experiments for the validation of soil moisture satellite data, both for the European Space Agency's Soil Moisture and Ocean Salinity and NASA's Soil Moisture Active Passive (SMAP) missions (she led the third SMAP Experiment). Since 2012, she has been responsible for the OzNet soil moisture monitoring network in the Murrumbidgee River catchment, as well as the CosmOz tower, Yanco, Australia. Her research areas include the estimation of soil moisture and vegetation parameters from airborne and ground-based L-band passive microwave observations, cosmic-ray probes, and Global Navigation Satellite Systems Reflectometry.